ACTA UNIVERSITATIS CAROLINAE
2003 GEOGRAPHICA, No. 2, PAG. 65–78

Meteorological Causes of Flood Situations in the Otava River Basin

JIŘÍ STEHLÍK†

Charles University in Prague, Faculty of Science
Department of Physical Geography and Geoecology

Abstract

Meteorological causes of floods have been analysed to understand relations between circulation types and resulting discharge values. The paper focuses on identification of pressure fields leading to extreme discharge values. Fields of surface air pressure are analysed in a long-term period. In meteorological terms, exceptionality of flood situations wasn't caused by special circulation types, but by two consecutive cyclones proceeding in a short time interval.

Key words: circulation types, pressure fields, meteorological causes of floods

1. Introduction

Hydrometeorological causes of flood situations in the Czech Republic have been studied by numerous authors, e.g. Buchtele (1972), Hladný (1995, 1996), Kakos (1973, 1985, 1997), Kakos and Štekl, (1998), Stehlík (2000), Vavruška (1989), Vilímek and Langhammer (2006), just to name a few.

This chapter specifies an automatic classification of circulation types (CTs) in the Otava river basin delimited by the profile in Písek. The main objective of the classification is to identify pressure fields that explain variability in the increase of discharge values. The classification involves daily values of surface air pressure fields recorded in 1899–2002, including the 2002 floods. Drawing on long-term statistics, we identify CTs preceding floods. In the time series of classified types, we search for days corresponding to the August flood. We compare circulation types with corresponding long-term statistical data and assess exceptional characteristics of meteorological situations in terms of classified CTs sequences.

2. Methodology

The purpose of the classification methodology applied in the study is to identify CTs explaining variability in discharge series, i.e. to define the types causing flood situations and the types with neutral effects. We build on data reflecting average daily discharge values in the Otava river basin down to Písek and values of surface air pressure in a regular nodal network of 5 x 5° over Europe and the eastern Atlantic. Data

on circulation were provided by the National Meteorological Centre for Atmospheric Research (NCAR). Data apply to geographical areas of 35°N – 65°N, 15°W – 40°E and the analysis covers the period from 1899 to 2002.

The discharge series was transformed by calculating remainders of discharge values recorded on the following days:

$$\Delta Q(t) = Q(t) - Q(t-1) \tag{1}$$

By transforming the series, we get positive values of $\Delta Q(t)$ applicable to the upward branch of the hydrograph and negative values applicable to the downward branch. As the main stress is put on periods with increasing discharge, negative values were replaced by zeros.

The CT classification methodology applied in the study represents a modification of methods described by Bárdossy, Stehlík, Caspary (2002). The classification is based on normalized pressure anomalies calculated daily in a regular node network, defining pressure anomalies spatial distribution for each CT. Pressure anomalies were calculated for each node point by deducting an average air pressure value applicable to a particular CT from an average value unconditional by a CT existence and dividing the resulting value by a standard deviation. The main benefit of working with air anomalies is the elimination of effects of annual air pressure changes: average values and standard deviations are calculated for each day of the annual cycle. In the course of classification, monitored (daily) circulation fields are compared with each of defined types. A CT showing the greatest conformity with the monitored field is selected as the circulation type of the particular day. As CT definitions aren't known in advance (as is the case in subjective classification), they have to be identified by optimisation. The target function that is maximised could be formally defined as follows:

$$O = \frac{1}{T}\sum_{t=1}^{T}\sum_{k=0}^{K}\left|\ln\left(1 - \frac{\Delta Q^{+}(CT(t-k))}{\overline{\Delta Q^{+}}}\right)\right| \tag{2}$$

where T is the number of days, $\Delta Q^{+}(CT(t-k))$ is the average increase in discharge applicable to a given CT, $\overline{\Delta Q^{+}}$ is the average increase in discharge independent of any CT. With respect to the lag of the flooding behind its causing situation, we work with a k period of preceding days. Due to the size of the monitored river basin, we define k as equal to 2 days. The optimisation method applied is known as simulated annealing (Aarts and Korst, 1989).

We also defined a "flood index" (PI) as a conditionality measure (j) of each CT occurrence in the period prior to a flood situation:

$$PI(CT) = \frac{n_1(CT)}{n_2(CT)} \tag{3}$$

where n_1(CT) is a relative frequency of a CT occurrence in the period prior to a flood and n_2(CT) is a relative frequency of the same CT occurrence independent of flood occurrence. The index is calculated separately for each annual season and for 1–10 days prior to a flooding. The PI values higher than one correspond to "flood" CTs – they appear in flood preceding periods more frequently than would be normal under unconditional circumstances.

In previous works (Stehlík J., 2002) we described a suitability test of applied input data variants that showed the best results when working with surface air pressure values. It isn't recommendable to use less than 10 CTs for classification purposes because we would lose data due to insufficient differences between particular situations and average weather conditions. Other studies work with 12 CTs, but in this case, the large amount of data allows for statistical processing of 14 CTs because they occurred in the past with a sufficient frequency.

3. Results

3.1. Pressure Fields of Circulation Types and Their Frequency

Applying the method briefly specified in chapter 2, we classify the time series of surface air pressure daily fields occurring in 1899–2002. Charts of pressure anomalies of all types are shown in Fig. 1. Negative anomalies are highlighted in blue and positive in red. The charts prove that the classification method provides a realistic output – high and low anomalies create compact areas. Individual CT frequencies are stated in Tab. 1.

Tab. 1 Frequency of individual circulation types in 1899–2002 [%]

CT	Spring	Summer	Autumn	Winter
1	5.66	5.75	7.05	6.13
2	6.04	5.41	3.94	4.92
3	9.41	10.05	9.56	10.07
4	4.38	4.89	4.86	4.95
5	4.29	5.3	4.89	4.25
6	3.92	4.37	5.58	4.22
7	8.67	9.98	8.81	10.28
8	7.04	8	8.51	7.87
9	5.67	5.98	7.54	6.23
10	15.64	13.63	10.95	13.1
11	4.79	4.24	3.52	4.12
12	7.93	8	9.01	8.13
13	5.27	4.76	5.69	5.34
14	8.45	7.66	7.84	8.15
unclass.	2.82	1.99	2.25	2.25

3.2. Circulation Types Flood Index

As the main flood criterion to assess the *PI* for all CTs, we established a threshold discharge value with a 1% probability of its overrun. The number of identified floods (Tab. 2) is logically lower than the number of days showing corresponding discharge values with the overrun probability specified above. This is because discharge values,

Fig. 1 Spatial distribution of average normalized pressure anomalies (1899–2002) for ground air pressure values for individual circulation types (CT)

identified during the analysis of the discharge value time series, equal to or higher than the threshold value shift the time series behind the flood thus identified, preventing repetitive involvement of the same flood in the *PI* calculation.

Tab. 2 Number of analysed flood events 1899–2002 [%]

Spring	Summer	Autumn	Winter
39	32	12	29

The *PI* index is calculated separately for each annual season. Results are summarised in Figs. 2–5. As the Figs. imply, the types with the highest *PI* values appearing in spring are CT 2, CT 11, CT 12, CT 9, in summer CT 9, CT 8, in autumn CT 2, CT 8, CT 9, and in winter CT 2, CT 11, CT 9.

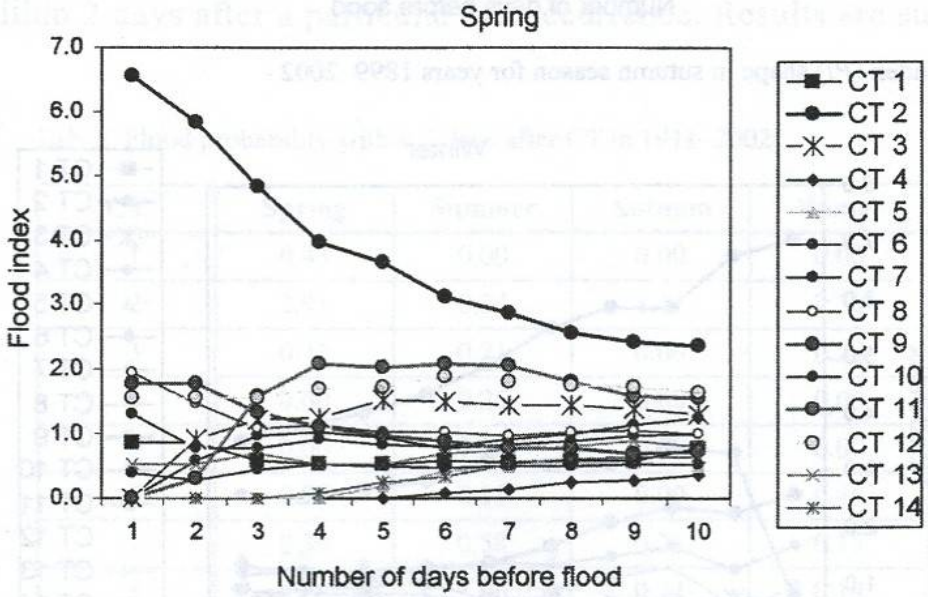

Fig. 2 Flood index (*PI*) shape in spring season for years 1899–2002

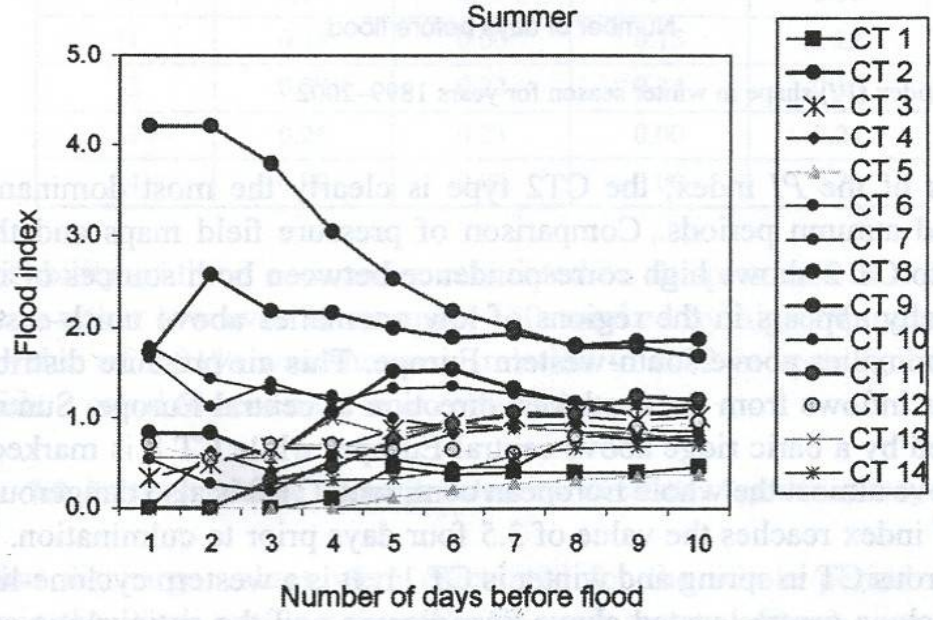

Fig. 3 Flood index (*PI*) shape in summer season for years 1899–2002

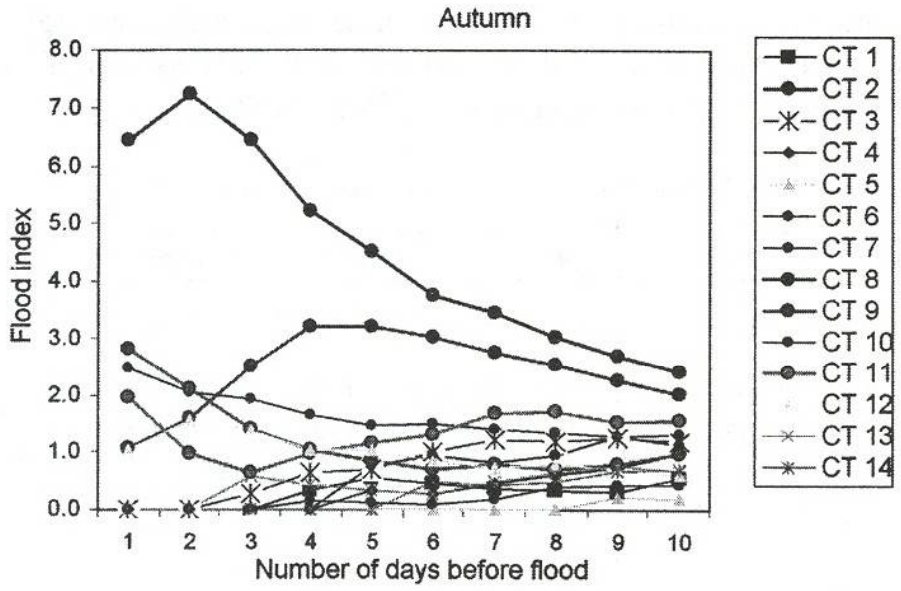

Fig. 4 Flood index (*PI*) shape in sutumn season for years 1899–2002

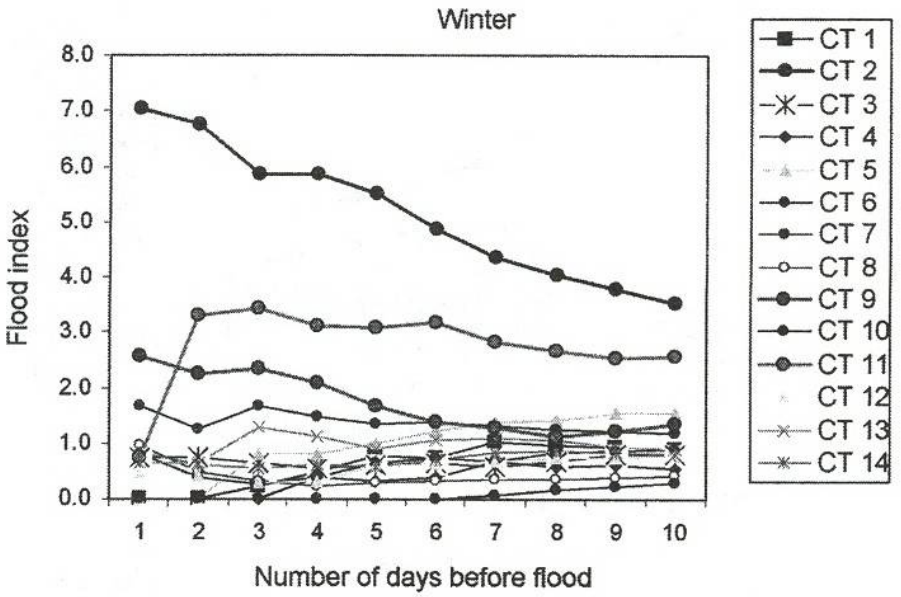

Fig. 5 Flood index (*PI*) shape in winter season for years 1899–2002

In terms of the *PI* index, the CT2 type is clearly the most dominant in spring, summer and autumn periods. Comparison of pressure field maps and the *PI* index applicable to CT 2 shows high correspondence between both sources of information. CT 2 typically appears in the regions of low anomalies above north-eastern Europe and high anomalies above south-western Europe. This air pressure distribution leads to humid air inflows from the northwest direction to central Europe. Summer CT 9 is characterised by a baric ridge above central Europe, while CT 8 is marked by a large cyclone above almost the whole European continent. CT 8 is also dangerous in autumn when its *PI* index reaches the value of 3.5 four days prior to culmination. The second most dangerous CT in spring and winter is CT 11. It is a western cyclone-like situation with the cyclone centre located above Scandinavia and the anticyclone centre above northern Africa.

Individual CT curves depicted by Figs. 2–5 imply that CT 2 is seven times more frequent 1–2 days prior to floods (with exception of summer periods) than would be normal under unconditional circumstances. In later stages (in case of longer periods prior to floods) the *PI* index falls down. To the contrary, the *PI* index applicable to CT 11 in spring ($PI = 2$) and in winter ($PI = 3$) remains constant with the exception of periods closely preceding flood situations. The same applies to CT 8 in summer ($PI = 2$) and winter ($PI = 3$).

Tab. 1 also implies that the frequency of flood CTs in various seasons is relatively high and therefore it is necessary to apply also a reverse procedure rather than calculate flood index values only on the basis of CT frequency linked to flood occurrence. The reverse procedure means to calculate flood probability on the premises of a particular CT occurrence.

Due to the time lag between causal situations and floods, we assume that flooding appears within 2 days after a particular CT occurrence. Results are summarised in Tab. 3.

Tab. 3 Flood probability within 2 days after CT in 1911–2002

CT	Spring	Summer	Autumn	Winter
1	0.43	0.00	0.00	0.00
2	2.91	0.34	1.11	2.50
3	0.46	0.21	0.00	0.28
4	0.00	0.25	0.00	0.00
5	0.00	0.00	0.00	0.00
6	0.30	0.11	0.00	0.46
7	0.39	0.58	0.31	0.15
8	0.73	1.06	0.24	0.18
9	0.89	1.72	0.32	0.83
10	0.14	0.45	0.00	0.00
11	0.15	0.00	0.15	1.22
12	0.77	0.22	0.24	0.16
13	0.26	0.23	0.00	0.24
14	0.00	0.00	0.00	0.23

The probability of flood occurrence calculated on the premises of a particular CT appearance is rather low even if we apply CTs marked by high *PI* index values (the maximum value of 2.91% was shown in relation to CT2 in spring), but the values shown in Tab. 3 equal to zero only in exceptional cases.

3.3. Trends in Extreme Discharge Values and Circulation Types Frequency

Maximum discharge values were calculated for the whole period of discharge monitoring in the Písek profile separately for each season of each year. Time series of discharge values and their tendency are specified in Fig. 6. Pursuant to the test of

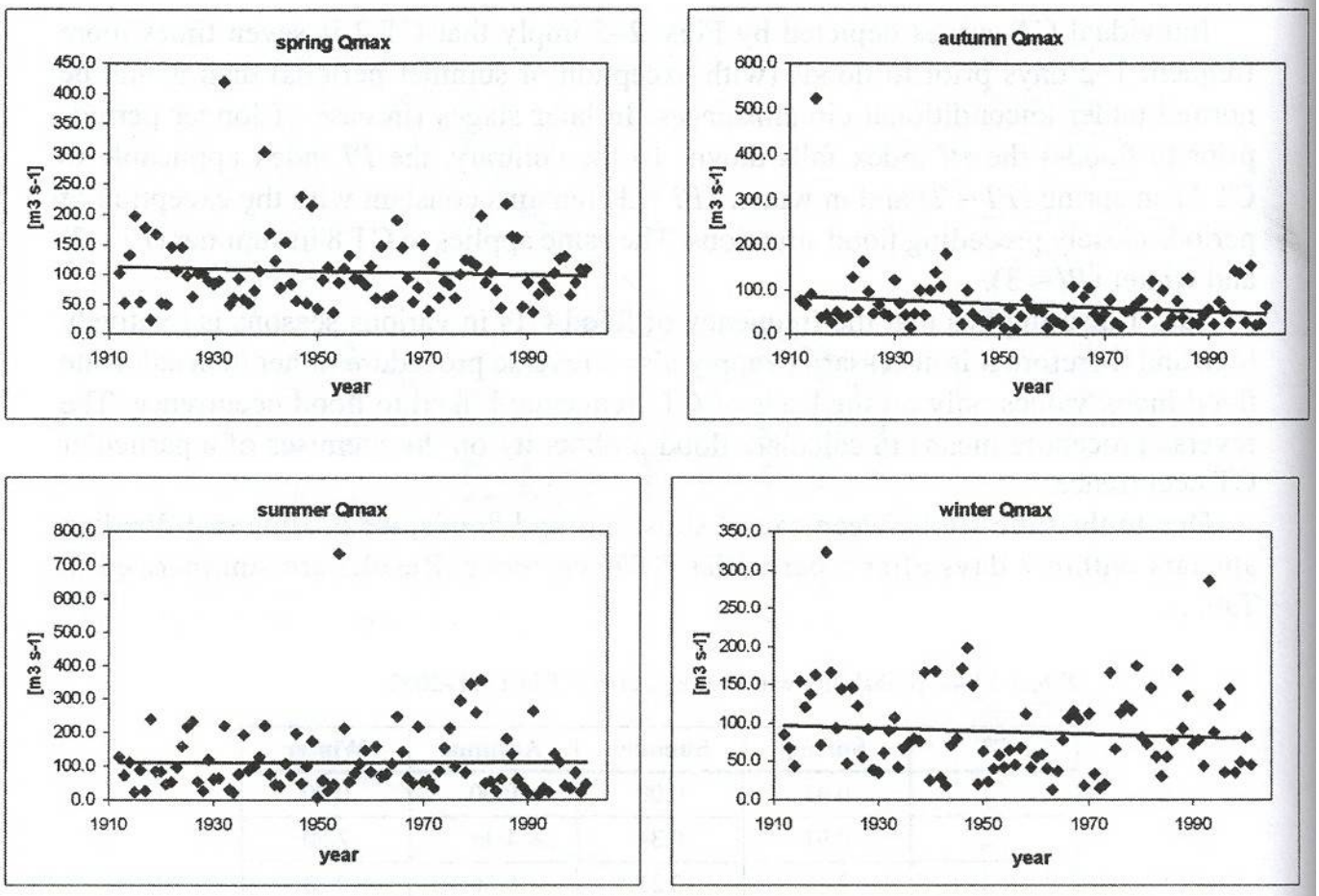

Fig. 6 Time series of seasonal maximal discharges with trendline

statistical significance, it was proved that at the significance level of $\alpha = 5\%$ none of calculated trends is significant (same results were acquired for maximum annual discharge values). This means that in the long-term the size of floods isn't reduced or enlarged in any season.

A similar analysis was performed in relation to CTs frequency. Results are summarised in Figs. 7–10. Tab. 4 shows CTs with trends labelled as statistically significant (again at the significance level of $\alpha = 5\%$).

Tab. 4 Circulation types marked by statistically significant trends

Spring	CT 5, CT 9, CT 13, CT 14
Summer	CT 2, CT 5, CT 9, CT 13, CT 14
Autumn	CT 2, CT 5, CT 9, CT 10, CT 14
Winter	CT 12

Constancy of flood discharge series is probably reflected also in the fact that most of CTs with significant trends don't belong among flood-inducing CTs. The only exception is CT 9 that appears quite frequently prior to floods in all seasons. However, significantly falling trend of this particular CT isn't sufficient to cause corresponding trends in peak discharge rates.

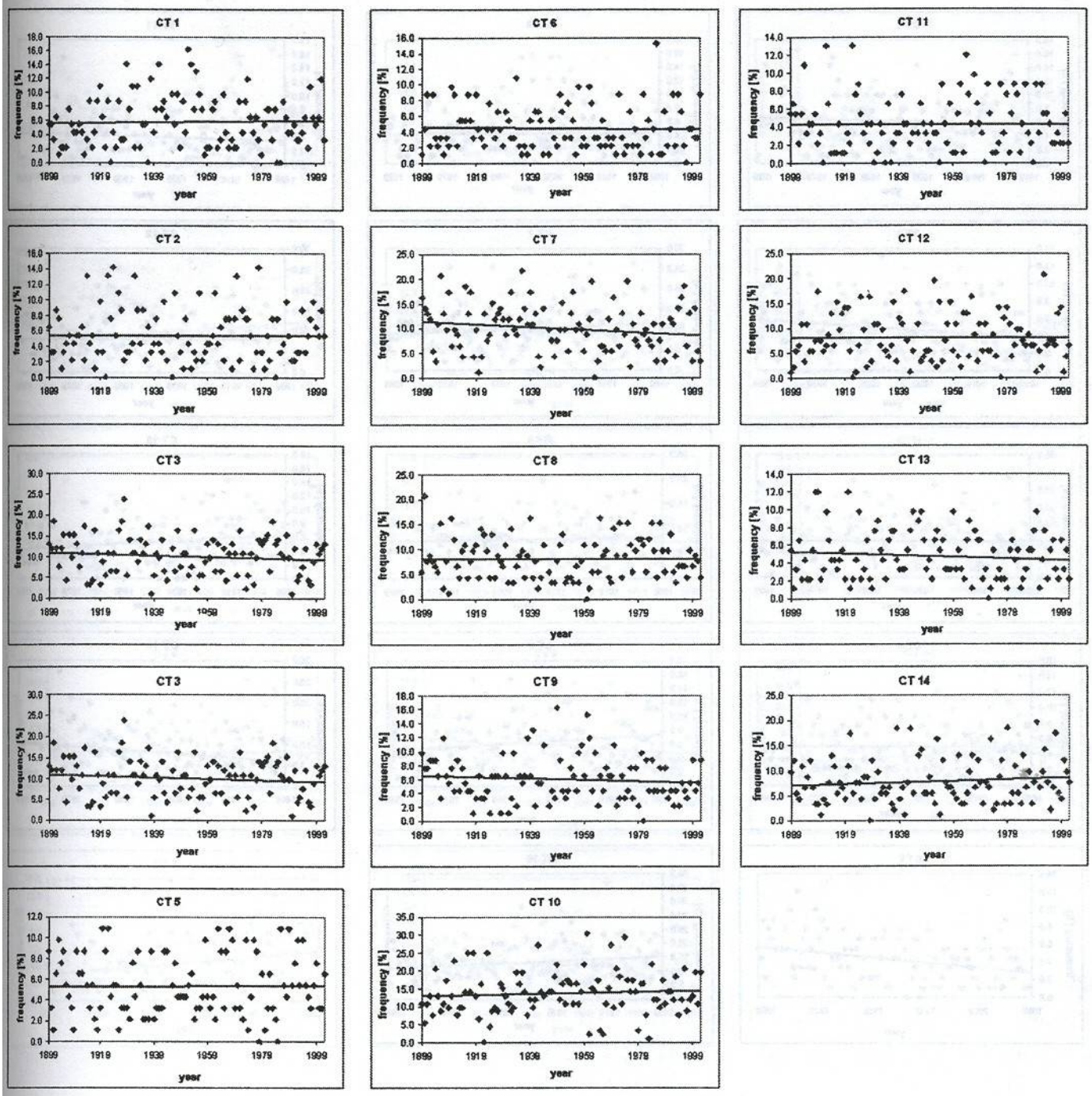

Fig. 7 CT frequencies with trendline (spring season)

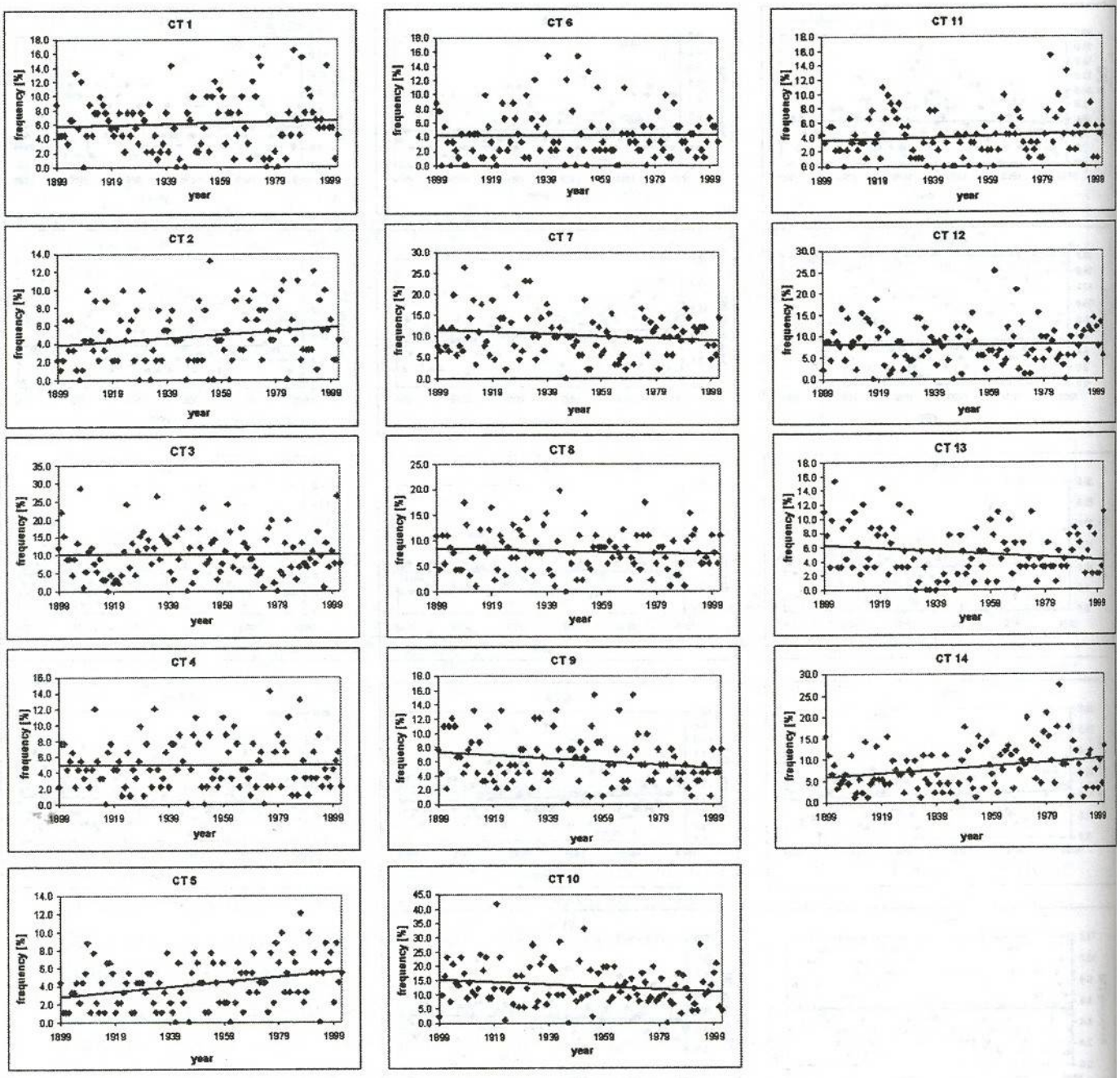

Fig. 8 CT frequencies with trendline (summer season)

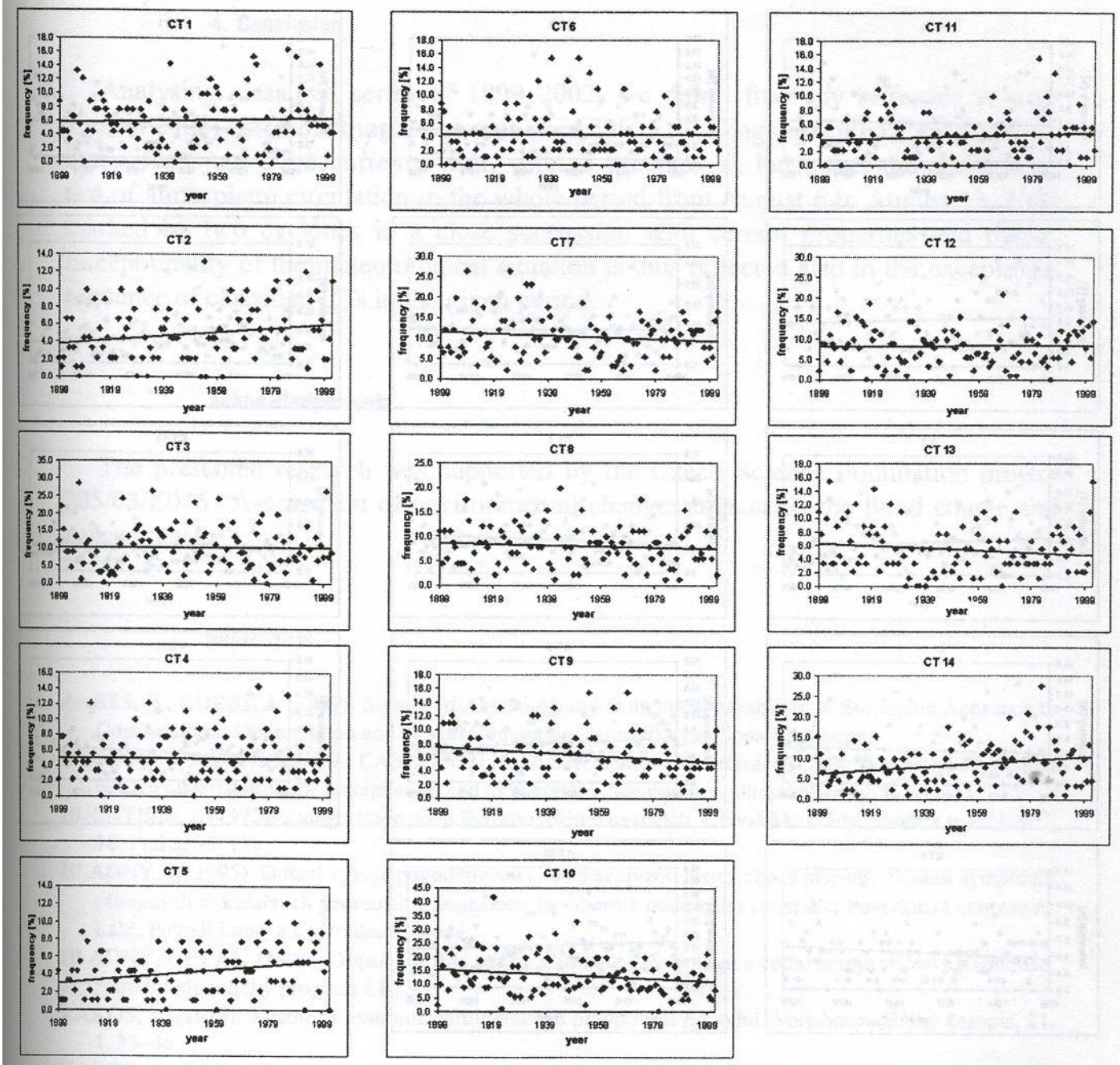

Fig. 9 CT frequencies with trendline (autumn season)

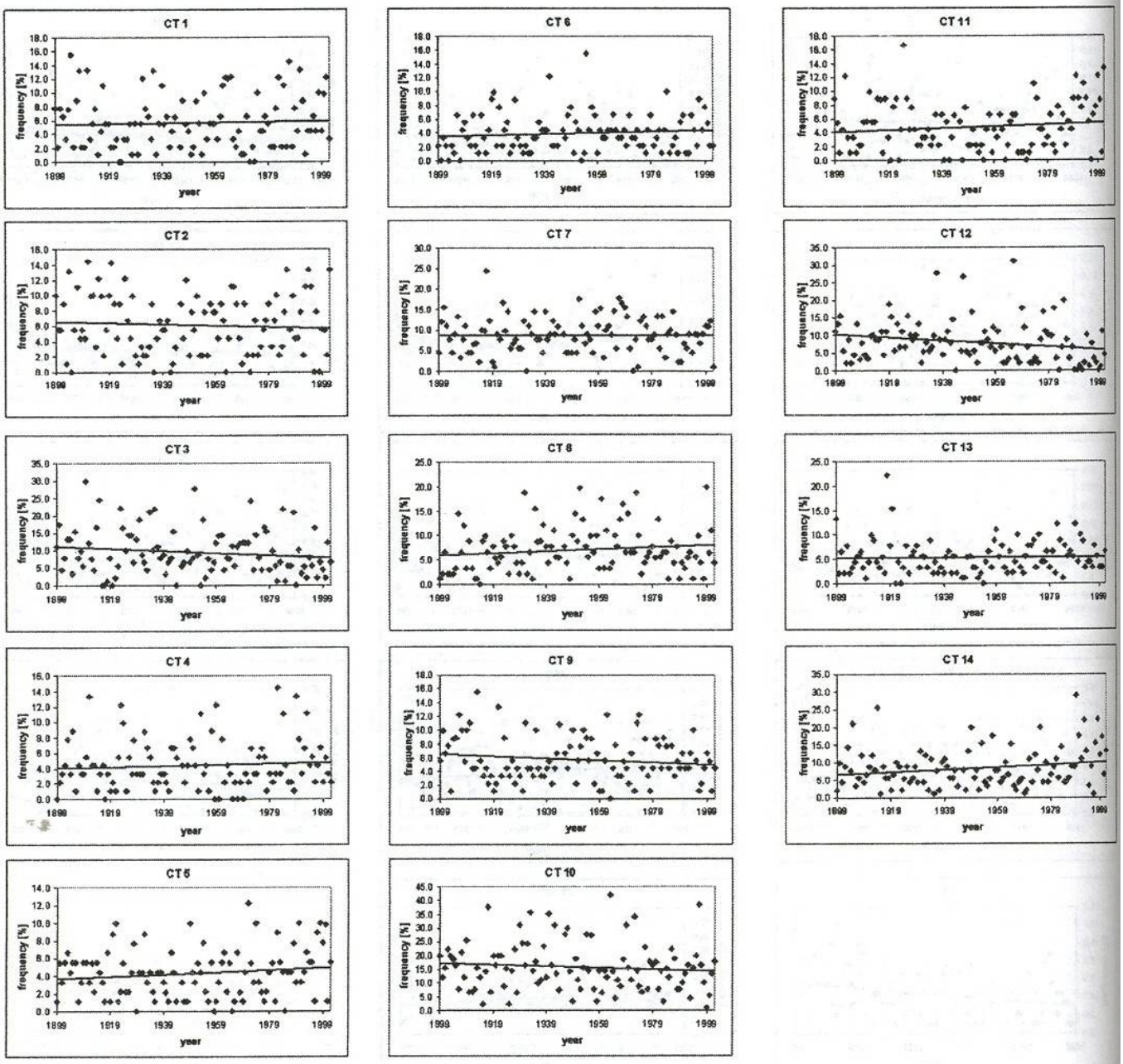

Fig. 10 CT frequencies with trendline (winter season)

3.4. Classification of Circulation Types Applicable to August 2002 Floods

Circulation types in the causal period of the August 2002 floods are listed in Tab. 5. Flood-inducing rains occurred on days classified as CT 8, CT 3, CT 2, and CT 9. In case of CT 8 and CT 9, such results are in line with long-term statistics of summer causal flood types (*PI* values).

Tab. 5 Classification of days of flood-inducing causal rains in August 2002 (days of extreme precipitation are marked by *)

day	*6. 8. 02**	*7. 8. 02**	*8. 8. 02*	*9. 8. 02*	*10. 8. 02*	*11. 8. 02**	*12. 8. 02**	*13. 8. 02**
CT	8	8	8	8	3	3	2	9

4. Conclusion

Analysing classified series of 1899–2002, we didn't find any sequence (except August 2002) corresponding to the section in Tab. 5. Findings specified above indicate that it isn't just CT occurrence itself what is exceptional, but rather the characteristics of atmosphere circulation in the whole period from August 6 to August 13, 2002 marked by two cyclones in a close succession with certain properties and tracks. Exceptionality of the meteorological situation is thus reflected also in the exceptional sequence of classified CTs in the given period.

Acknowledgements

The presented research was supported by the Czech Science Foundation project 205/03/Z046 "Assessment of environmental changes impact on the flood course and consequences".

References

AARTS, E., KORST, J. (1989): Simulated Annealing and Boltzmann Machines: A Stochastic Approach to Combinatorial Optimization and Neural Computing. John Wiley & Sons, Chichester.

BÁRDOSSY, A., STEHLÍK, J., CASPARY, H. J. (2002): Automated optimized fuzzy rule based circulation pattern classification for precipitation and temperature downscaling. Climate Research, 23, 1, 11–22.

BUCHTELE, J. (1972): Kategorizace povodňového režimu na tocích Vltavské kaskády. Sborník prací HMÚ, 18, Praha, 65–139.

HLADNÝ, J. (1995): Odhad vývoje povodňových situací analýzou historických případů. Soubor symptomů příčinných cirkulačních podmínek v atmosféře. In: Sborník odborného semináře: Povodňová ochrana na Labi, Povodí Labe, a.s., Hradec Králové.

HLADNÝ, J. ET AL. (1996): Dopady možné změny klimatu na hydrologii a vodní zdroje v České Republice, Národní klimatický program ČR, 20.

KAKOS, V. (1973): Možnosti hydrometeorologických předpovědí povodní. Vodohospodářský časopis, 21, 1, 33–46.

KAKOS, V. (1985): Hydrometeorologická analýza povodňových situací v povodí Labe. Meteorologické zprávy, 38, 5, ČHMÚ, Praha, 148–151.

KAKOS, V. (1997): Hydrometeorologická analýza historické povodně v roce 1897 ve vztahu ke katastrofálním záplavám v Čechách a na začátku září 1890 a na Moravě v červenci 1997. Meteorologické zprávy, 50, 191–196.

KAKOS, V., ŠTEKL, J. (1998): Posouzení výjimečnosti hydrosynoptické situace na základě srovnání s dostupnými historickými případy. Ústav fyziky atmosféry AV ČR, Praha.

STEHLÍK, J. (2000): Klasifikace povětrnostních situací pro potřeby hydrometeorologických analýz. Sborník konference Hydrologické dny 2000, Nové podněty a vize pro příští století, Plzeň, p. 75–82.

VAVRUŠKA, F. (1989): Meteorologické příčiny povodní na Otavě a Lužnici. Meteorologické zprávy, 42, 4, ČHMÚ, Praha, 111–115.

VILÍMEK, V., LANGHAMMER, J. (2006): Assessment of Flood Course and Consequences. Acta Univ. Carol., Geographica, 38, 2, p. 203–217.

http://dss.ucar.edu/datasets/ds010.0/ Daily (and Monthly) Northern Hemisphere Sea Level Pressure Grids, continuing from 1899.

Résumé

V práci je na základě metodiky Bardóssyho a kol. (2002) provedena automatická objektivní klasifikace povětrnostních situací (cirkulačních typů – CT) pro povodí Otavy. Metoda využívá přízemních tlakových polí nad Evropou a severním Atlantikem (v prostoru 35°N–65°N, 15°W–40°E) poskytnutých National Meteorological Centre for Atmospheric Research (NCAR) za období 1899 až 2002.

Bylo provedeno rozdělení cirkulačních polí na 14 typů definovaných na základě pozitivních a negativních odchylek tlaku od dlouhodobých hodnot, přičemž jsou zohledněny i sezónní vlivy. Pro každý den je pak identifikován příslušný cirkulační typ na základě nejlepší shody s definovanými CT.

Z řady denních průměrných průtoků v závěrovém profilu Otavy, v Písku, byly spočteny denní přírůstky (poklesy nejsou uvažovány). Přitom pro povodně – pro dny s pozitivním přírůstkem a s průměrným denním průtokem s pravděpodobností dosažení 1% (v použité průtokové řadě) – byly identifikovány CT dva dny před událostí, které jsou považovány za příčinné. Pro všechny CT byl vypočten „povodňový index" *PI*:

$$PI(CT) = \frac{n_1(CT)}{n_2(CT)}$$

kde n_1(CT) je relativní četnost výskytu daného CT před povodní a n_2(CT) je celková četnost výskytu daného CT ve zkoumaném období. Hodnoty *PI* větší než jedna příslušejí „povodňovým" CT: ty se vyskytují v daném období před povodní častěji, než by odpovídalo jejich nepodmíněné četnosti výskytu.

Jako „povodňově nebezpečné" typy byly identifikovány zejména CT2 pro jaro, podzim a zimu, CT9 pro letní období, dále také CT11 pro zimu a jaro a CT8 pro léto a podzim. Zároveň však z dalšího provedeného vyhodnocení vyplývá, že pravděpodobnost výskytu povodně i po povodňových CT je relativně malá a dosahuje maximálně 2,91 % v případě CT2 a jarního období a 1,72 % pro CT9 v létě. Pro CT2 je typická oblast záporných anomálií nad severovýchodní Evropou a kladných anomálií nad Evropou jihozápadní. Toto rozložení tlaku vzduchu má za následek příliv vlhkého vzduchu ze severozápadního směru do prostoru střední Evropy. CT9 je charakterizován přítomností barického sedla nad prostorem střední Evropy. Pro CT8 je typická rozsáhlá tlaková níže pokrývající téměř celý evropský kontinent. CT11 s tlakovou níží nad Skandinávií a výší nad severní Afrikou způsobuje zonální západní proudění.

Při rozboru hodnot maximálních ročních ani sezónních průtoků nebyl pozorován žádný signifikantní trend přírůstku či poklesu, stejně jako u pravděpodobnosti výskytu většiny CT.

V případě extrémní povodně ze srpna 202 bylo provedeno podrobnější hodnocení potvrzující výskyt „povodňových" CT před oběma epizodami povodně. Rozbor řady CT ukazuje, že výjimečný není výskyt jednotlivých CT sám o sobě, ale povaha cirkulace atmosféry v celém období 6. 8.–13. 8. 2002, pro které je charakteristická následnost dvou po sobě jdoucích tlakových níží s danými vlastnostmi a trajektoriemi.

Author's full address:
JIŘÍ STEHLÍK †
Charles University in Prague, Faculty of Science
Department of Physical Geography and Geoecology
Albertov 6, 128 43 Prague 2